Carbohydrate Polymers 75 (2009) 566–574

Contents lists available at ScienceDirect

Carbohydrate Polymers

journal homepage: www.elsevier.com/locate/carbpol

Preparation of aspirin and probucol in combination loaded chitosan nanoparticles and in vitro release study

Wan Ajun [a,*], Sun Yan [a], Gao Li [b], Li Huili [c,*]

[a] School of Chemistry & Chemical Technology, Shanghai Jiao Tong University, 800 Dongchuan Road, Shanghai 200240, China
[b] School of Resource and Environment, Ningxia University, 539 Henanshan Road(w), Yinchuan 750021, China
[c] School of Pharmacy, Shanghai Jiao Tong University, 800 Dongchuan Road, Shanghai 200240, China

ARTICLE INFO

Article history:
Received 16 July 2007
Received in revised form 25 February 2008
Accepted 27 August 2008
Available online 6 September 2008

Keywords:
Aspirin
Probucol
Chitosan nanoparticles
Combination load
In vitro release

ABSTRACT

We design and develop chitosan nanoparticles which load two different drugs simultaneously. Aspirin (acetylsalicylic acid, ASA), a hydrophilic drug and probucol (PRO), a hydrophobic drug, are chosen as typical drugs, which are widely used to treat restenosis. The drug loaded chitosan nanoparticles are prepared by gelation of chitosan with tripolyphosphate (TPP) by ionic cross-linking. The physicochemical properties of nanoparticles are investigated by FTIR, transmission electron microscope (TEM), scanning electron microscopy (SEM) and differential scanning calorimetry (DSC). The images show that these particles are spherical in shape with ASA being in the amorphous phase, while PRO is crystalline. The properties of chitosan nanoparticles such as encapsulation capacity and controlled release behaviors of ASA and PRO are evaluated. Experimental results indicate that the loading capacity (LC), encapsulation efficiency (EE) and ASA and PRO release behaviors are affected by several factors including pH, concentration of TPP, chitosan molecular weight (MW) and ASA initial concentration as well as PRO. In vitro release shows that the nanoparticles provide a continuous release. Entrapped ASA is released for more than 24 h and PRO lasts longer for 120 h.

1. Introduction

Percutaneous transluminal coronary angioplasty (PTCA) is a promising method for curing obstructed coronary artery disease. PTCA procedures include balloon dilation, excisional atherectomy, endoluminal stenting and laser ablation (Baim, 1992). However, revascularization induces thrombosis and neointimal hyperplasia, which in turn cause restenosis in 30–40% of coronary arteries within 6 months after successful balloon angioplasty (Nobuyoshi, Kimura, & Ohishi, 1991). Patients undergoing PTCA require additional surgical intervention because of a combination of factors including elastic recoil, thrombosis, vessel remodeling, local tissue inflammation and neointima formation (Currier & Faxon, 1995). In general, the pathogenesis of restenosis is multifactorial. What is more, the patients, suffering restenosis, show several symptoms than could be controlled by employing multidrugs. So combination dosing is usually adopted in clinical therapy. There are a variety of drugs (e.g. aspirin, probucol, rapamycin) which are used for clinical treatment. Aspirin (ASA) as a hydrophilic drug is often used due for its anti-atherosclerotic effect (Kato et al., 2005). Probucol (PRO), a hydrophobic drug may prevent restenosis by exerting an anti-oxidative effect (Watanabe, Sekiya, Ikeda, Miyagawa, & Hashida, 1996). As common drugs used in anti-restenosis, ASA and PRO chosen in this study.

Furthermore, an effective anti-restenotic therapy should combine sufficiently high and sustained drug levels at the injury site with minimal systemic and local toxicity (Banai et al., 2005). Drug loaded nanoparticles offer the advantage of high tissue uptake and protracted drug residence at the injury site (Banai et al., 1998; Fishbein et al., 2000, 2001; Guzman et al., 1996). There has been considerable interest in developing chitosan nanoparticles as effective drug delivery devices (Janes, Calvo, & Alonso, 2001). Chitosan is a linear polysaccharide containing two β-1,4-linked sugar residues, *N*-acetyl-D-glucosamine and D-glucosamine, distributed randomly along the polymer chain. It is obtained commercially by partial de-*N*-acetylation of chitin (Thierry, Winnik, Merhi, Silver, & Tabrizian, 2003). It is a biodegradable, biocompatible, naturally occurring polymer. Chitosan is one of the major components used in vascular surgery, tissue culture and tissue regeneration as a hemostatic agent (Kolhe & Kannan, 2003; Li, Yun, Gong, Zhao, & Zhang, 2006). Chitosan scaffolds have been investigated for use in tissue engineering (Madihally & Matthew, 1999). Even though the discovery of chitosan dates from the 19th century, it has only been over the last two decades that this polymer has received attention as a material for biomedical and drug delivery applications because of its desirable biological properties.

* Corresponding authors. Tel.: +86 21 34201245; fax: +86 21 54741297.
E-mail addresses: wanajun@sjtu.edu.cn (W. Ajun), lihl@sjtu.edu.cn (L. Huili).

0144-8617/$ - see front matter © 2008 Elsevier Ltd. All rights reserved.
doi:10.1016/j.carbpol.2008.08.019

Chitosan nanoparticles showed high cytotoxic activity toward tumor cells, while low toxicity against normal human liver cells (L-02) (Qi, Xu, Jiang, Li, & Wang, 2005). Chitosan nanoparticles show high sorption capacity and anti-bacterial activity (Qi & Xu, 2004; Qi, Xu, Jiang, Hu, & Zou, 2004). The unique cationic character of chitosan nanoparticles could provide higher affinity with negatively charged biological membranes and site-specific targeting in vivo (Qi et al., 2004). Particle size also substantially increases their anti-tumor efficacy when chitosan nanoparticles are applied by intravenous injection (Qi et al., 2005). The unique character with positive charge and small particle size of chitosan nanoparticles is responsible for their in vivo efficacy (Qi & Xu, 2006). Moreover, it is reported that chitosan can suppress the proliferation of vascular smooth muscle cells, consequently, preventing restenosis of rabbit (Joseph, 2006; Lim et al., 2005). Therefore, drug loaded chitosan nanoparticles might be valuable in the treatment of restenosis.

In this paper, we report the study of the drug release behavior of ASA/PRO from nanoparticles, ASA and PRO combined loaded chitosan nanoparticles have been prepared based on an ionic gelation process. We have characterized and compared the properties of chitosan nanoparticles loaded with combined drugs under different preparation conditions, pH value and concentration of TPP. The drugs in vitro release, LC and EE of drugs are also explored with a view to understanding the effects of pH and concentration of TPP on molecular interactions interactions between the two drugs. Thus, we can modulate their encapsulation capability and release rate by adjusting the molecular and formation parameters.

2. Materials and methods

2.1. Materials

Chitosan with different MW (21, 40, 67 kDa and degree of deacetylation was 90%) are obtained from Dacheng Biotech. Co. Ltd. (Weifang, People's Republic of China). Aspirin is obtained from Lunan Pharmaceutical Co. Ltd. (Linyi, China). Probucol is from Qilu Pharmaceutical Co. Ltd. (Jinan, China). Sodium tripolyphosphate (TPP) and other reagents are all of analytical grade.

2.2. Preparation of ASA and PRO combined drugs loaded chitosan nanoparticles

Chitosan solutions (2.5 mg/mL, 25 mL) are prepared by dissolving chitosan in 1% acetic acid. ASA is added into the solution with different concentration (0.8, 1.0 and 1.2 mg/mL). After dissolving completely, Tween-80 (2% v/v) is added as a surfactant. PRO (7.5, 10.0 and 12.5 mg) is dissolved in CH_2Cl_2 and then this oil phase is mixed with aqueous phase (chitosan solution contained aspirin) by stirring vigorously for 20 min. CH_2Cl_2 is chosen because of its ability to diffuse into the aqueous phase at a rapid rate facilitating particles formation upon evaporation. The ratio of oil and aqueous phase is 1:10. TPP solution (10 mL) is dropped into O/W emulsion under magnetic stirring. After 1 h of cross-linking, nanoparticles are isolated by centrifugation at 9000 rpm for 30 min.

2.3. Morphological characterization

The surface morphology of nanoparticles is observed by TEM and SEM. For TEM, the nanoparticles solution is dropped on copper grids and dried overnight at room temperature for viewing (JEM-100CX, JEOL, Japan). Samples of frozen dried nanoparticles are mounted on metal stubs, gold coated under vacuum and then examined on a S-2150 SEM (Hitachi, Japan).

2.4. FTIR analysis

The nanoparticles solution is centrifuged at 9000 rpm for 30 min. Supernatants are discarded and drug loaded chitosan nanoparticles are freeze-dried for 24 h at −34 °C, followed by a gradual increase in temperature until 20 °C, using a BETA1-8 freeze-dryer (BETA, N/A) ($n = 3$). The IR spectrum of samples is recorded on a Fourier Transform Infrared Spectrometer 430 (Perkin-Elmer, USA).

2.5. DSC analysis

A differential scanning calorimeter (DSC), Model Perkin-Elmer PYRIS I, was used. Each freeze-dried sample (5–10 mg) is run at a scanning rate of 10 °C/min under nitrogen atmosphere. The temperature for the scan ranged from 20 to 180 °C.

2.6. Evaluation of drug loading efficiency

The encapsulation efficiency and loading capacity of nanoparticles are determined by the separation of nanoparticles from the aqueous medium containing free drug by centrifugation at 9000 rpm for 30 min. The amount of free ASA and PRO in the supernatant is measured with a spectrophotometer at 242 and 298 nm, separately. Dilutions of samples and calibration curves are performed in phosphate buffered saline (PBS pH 7.4). The encapsulation efficiency ($EE_{1,2}$) and loading capacity ($LC_{1,2}$) of ASA and PRO of the nanoparticles are calculated as follows:

$$EE_{1,2} = \frac{T_{1,2} - F_{1,2}}{T_{1,2}} \times 100, \quad LC_{1,2} = \frac{T_{1,2} - F_{1,2}}{W_N} \times 100$$

$T_{1,2}$ are total amount of ASA and PRO. $F_{1,2}$ are amount of free ASA and PRO. W_N is the nanoparticles weight. All measurements are performed in triplicate.

2.7. Evaluation of in vitro drug release

The ASA and PRO combined drugs loaded nanoparticles separated from 18 mL suspension are placed into test tubes with 6 mL of 0.2 mol/l phosphate saline cushion liquid (PBS), and incubated at 37 °C under stirring. At varying time points, supernatants are isolated by centrifugation. Samples (3 mL) are removed and replaced by fresh medium with the same volume. The amount of released ASA and PRO are analyzed with spectrophotometer (PE, America) at 298 and 242 nm, respectively.

2.8. Statistical analysis

All experiments are repeated a minimum of three times and measured in triplicate. Results reported are means ± SD, unless otherwise noted. Statistical significance is analyzed using Student's *t*-test. Differences between experimental groups are considered significant when *P*-value is less than 0.05.

3. Results and discussion

3.1. Formation and characterization of combined drugs loaded chitosan nanoparticles

The preparation of chitosan nanoparticles, based on an ionic gelation process, involves the mixture of two different phases at room temperature. One phase is an aqueous phase of acetic acid solution containing chitosan and ASA. The other phase is an oil

phase of CH_2Cl_2 containing PRO. An O/W emulsion forms after mixing the two phases. After adding TPP solution, nanoparticles form immediately through inter and intramolecular linkages created between TPP phosphates and chitosan amino groups. The molecular structures of ASA, PRO, TPP and chitosan, are shown in Fig. 1. Some ASA is embedded in nanoparticles and some is adsorbed on the surface of the particles because of the electrostatic interaction between amino groups of chitosan and carboxyl of ASA. PRO is hydrophobic, which can be entrapped into nanoparticles by being dissolved in CH_2Cl_2 prior to its incorporation into the chitosan solution, followed by the addition of the TPP solution.

Fig. 2 shows FTIR spectra of ASA, PRO, chitosan and combined drugs loaded chitosan nanoparticles. The absorption band at 1595 cm^{-1} is ascribed to N–H bending mode in the primary amine of chitosan (Fig. 2C), but it disappears in drug loaded chitosan nanoparticles (Fig. 2D), which could be attributed to the linkage between tripolyphosphoric groups of TPP and ammonium groups of chitosan in nanoparticles (Knaul, Hudson, & Creber, 1999). Pure PRO spectra shows sharp characteristic peaks at 2959, 1423 and 1309 cm^{-1} (Fang et al., 1999). All the above characteristic peaks appear in the spectra of combined drugs loaded chitosan nanoparticles (Fig. 2D) at the same wavenumber indicating no modification or interaction between the drug and carrier. 1757, 1690 and 1606 cm^{-1} assign to $\nu_{C=O}$ (acetoxy group), $\nu_{C=O}$ (carboxylic group) and skeletal in-plane vibration of aromatic ring of ASA, respectively (Fig. 2A). The characteristic absorption peaks of ASA at 1757 cm^{-1} (acetoxy group), and 1690 cm^{-1} (carboxylic group) shifts to 1644 and 1540 cm^{-1}, respectively (Fig. 2D), which are due to the interaction between intermolecular OH...O=C and HNH...O=C bonds with participation of carboxylic COOH of ASA and primary amide of chitosan (Koleva, 2006). Characteristic absorption peak of ASA at 1606 cm^{-1} is overlapped with 1644 cm^{-1}. The results indicate that PRO and ASA together have been loaded successfully into the chitosan nanoparticles.

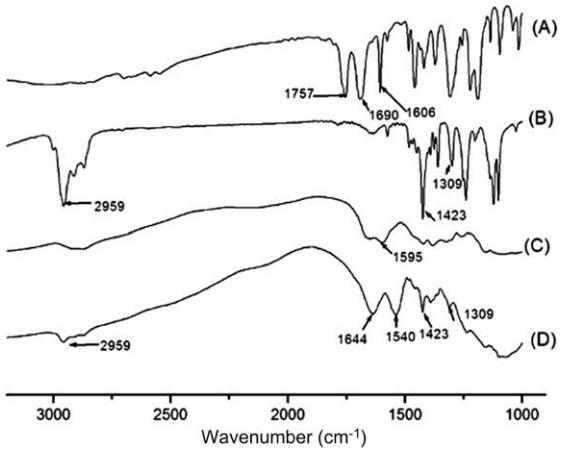

Fig. 2. FTIR of ASA (A), PRO (B), chitosan (C) and combined drugs loaded nanoparticles (D).

TEM and SEM images of combined drugs loaded chitosan nanoparticles are show in Figs. 3 and 4, respectively. Fig. 3 shows that

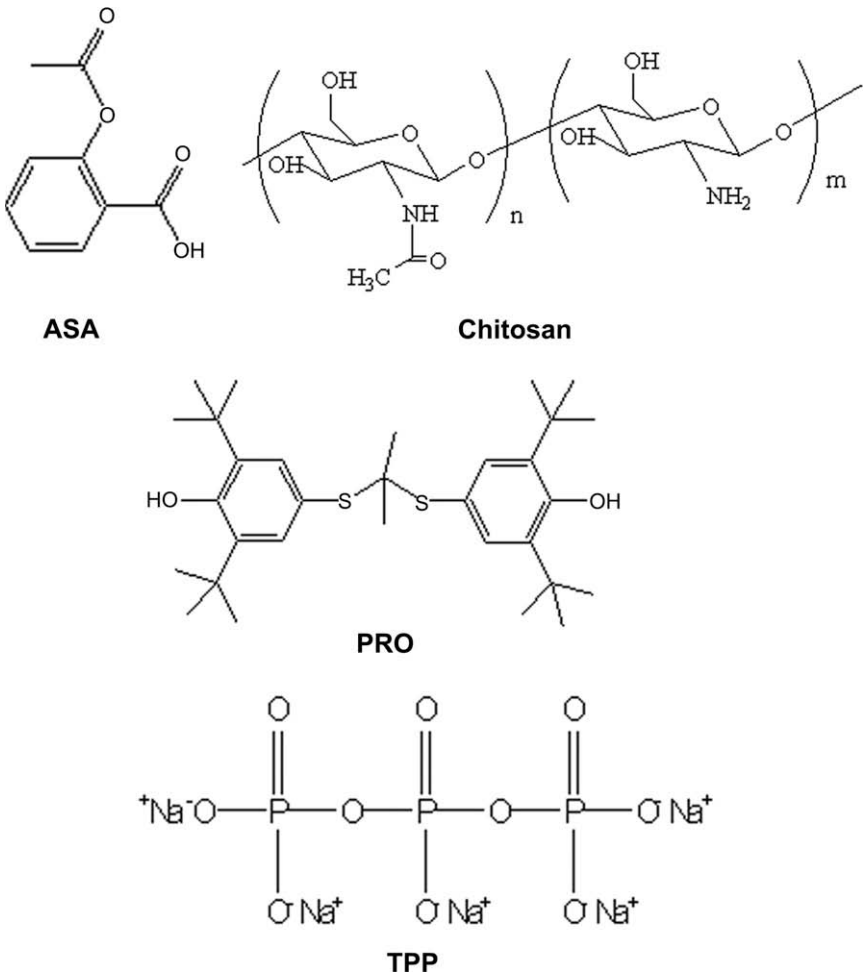

Fig. 1. Chemical structures of ASA, PRO, TPP and chitosan.

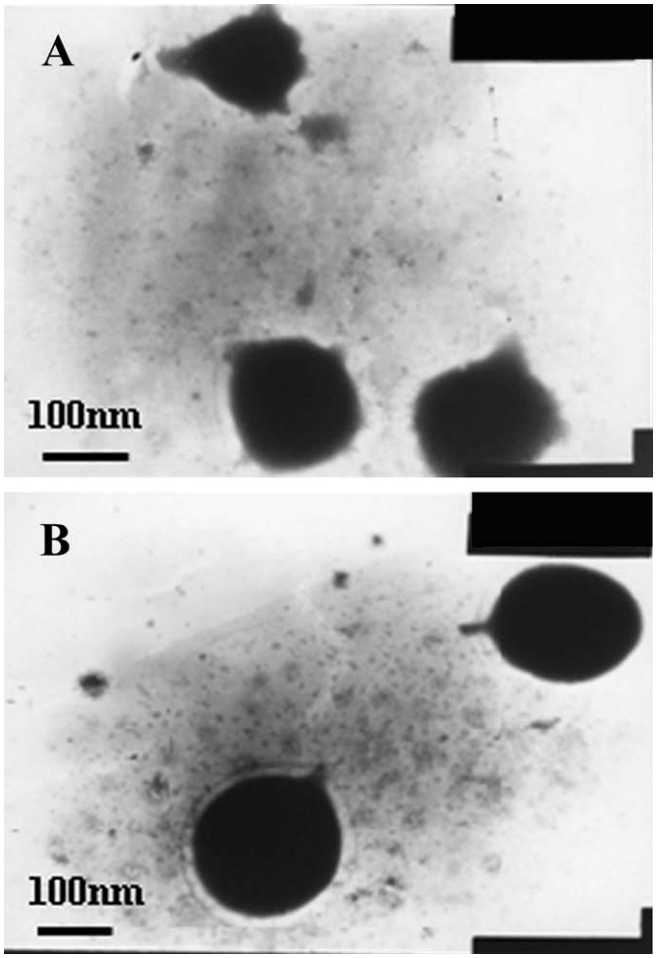

Fig. 3. TEM images of combined drugs loaded chitosan nanoparticles with different TPP concentration: (A) TPP1.0 mg/mL, (B) TPP2.5 mg/mL.

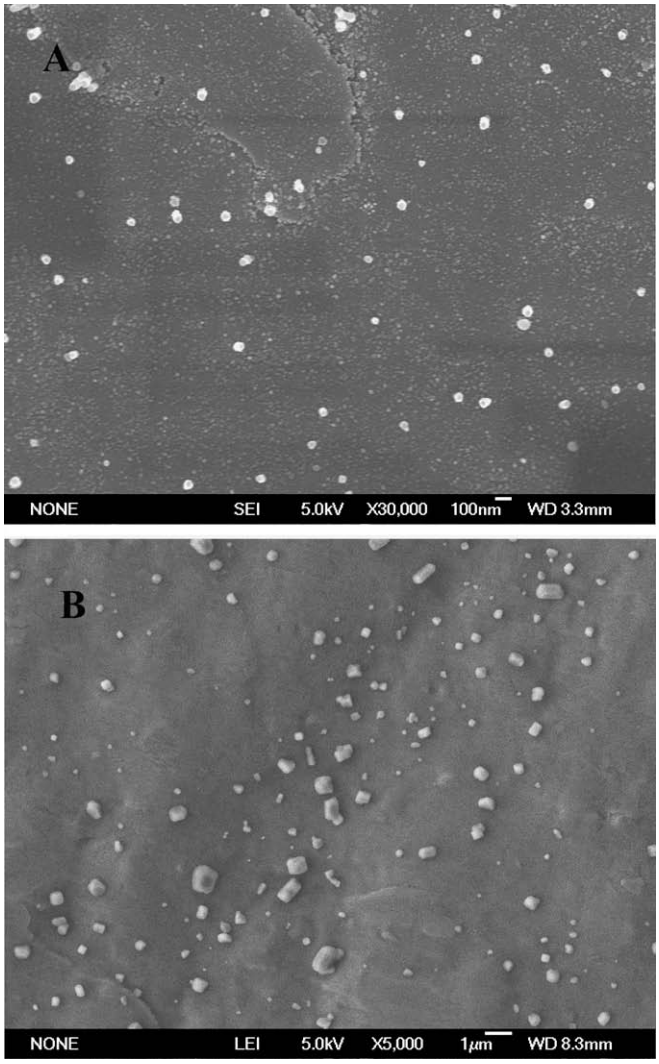

Fig. 4. SEM images of combined drugs loaded chitosan nanoparticles with different TPP pH: (A) pH 3, (B) pH 7.

the particle size increases with increasing TPP concentration. At the low TPP concentration (1.0 mg/mL) (Fig. 3A), combined drugs loaded chitosan nanoparticles are in the size range from 100 to 200 nm; when TPP concentration is 2.5 mg/mL (Fig. 3B), the average particle size slightly increases to about 200–300 nm. These results would be due to stiffness of the cross-linkage between TPP and chitosan, as the increase of TPP concentration, there would be more tripolyphosphoric ions to cross-link with amino groups on chitosan chains (Calvo, Remuñán-López, Vila-Jato, & Alonso, 1997).

TPP-chitosan microparticles are prepared by the ionic interaction between a positively charged amino group of chitosan and a negatively charged counterion of TPP. The ionization degree of TPP is dependent on the pH value of solution. The pH value of TPP solution affects the morphology of nanoparticles surface and particle size observably (Ko, Park, Hwang, Park, & Lee, 2002). Fig. 4 shows the morphology of combined drugs loaded chitosan nanoparticles prepared with different pH values of TPP solution. Nanoparticles prepared with pH 3 TPP solution (Fig. 4A) are spherical in shape, and have smooth surfaces and the size of nanoparticles is under 100 nm. When TPP is pH 7 (Fig. 4B), the combined drugs loaded chitosan nanoparticles are not completely spherical in shape, and have rough surfaces. In addition, the diameters of the combined drugs loaded chitosan nanoparticles are between 200 nm and 1 μm, which shows that after loading the combined drugs, chitosan cross-linked with TPP at a higher pH value (pH 7) results in a broader size distribution. The ionization degree of TPP is dependent on the pH value of solution. Chitosan nanoparticles prepared in acidic TPP solution are completely ionic cross-linking dominated (Lee, Mi, Shen, & Shyu, 2001; Mi, Shyu, Lee, & Wong, 1999b; Mi et al., 1999a). At low pH, only $P_3O_{10}^{5-}$ anions are found in TPP solution. Moreover, chitosan is a weak polybase, as the pH of the solution decreases, the ionization of the amine group of chitosan increases. In high pH solutions, TPP is dissociated into OH^- and TPP ions ($HP_3O_{10}^{4-}$ and $P_3O_{10}^{5-}$). However, in these high pH solution, the ionization of amine group of chitosan decreases. Therefore, with low or high pH value TPP solution, the cross-link between chitosan and TPP could be more complete. The structure of the nanoparticles would be more compact and also the surface would be smoother.

Combined drugs loaded chitosan nanoparticles are analyzed by DSC in order to try and characterize the physical forms of the drugs in the polymer and to investigate for intermolecular interactions (Broman, Khoo, & Taylor, 2001). PRO has been reported as having at least two polymorphs with onset melting points of 116 °C (Form II) and 125 °C (Form I), where the Form I polymorph is the thermodynamically stable form (Gerber, Caira, & Lotter, 1993). Form II is prepared by rapid crystallization from a concentrated solution in ethanol and has a melting point of 116 °C (Gerber et al., 1993). The material as received is found to have melting point of 125 °C

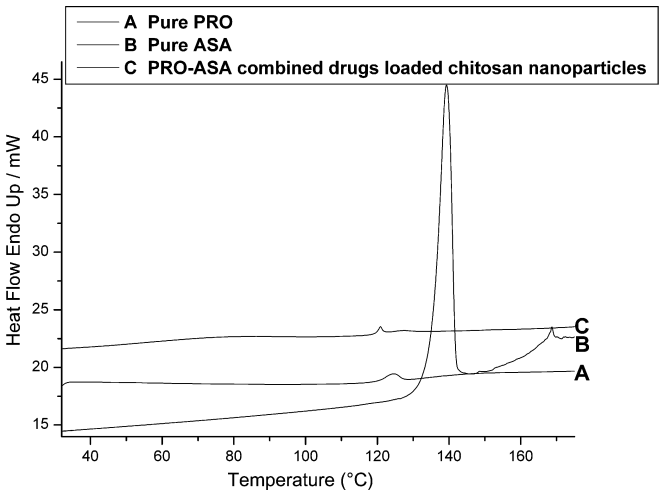

Fig. 5. DSC thermograms of pure PRO (A), pure ASA (B) and RPO–ASA combined drugs loaded chitosan nanoparticles (C).

as measured by DSC (Fig. 5A) and is thus Form I. Most recently, computational studies have addressed polymorphism in ASA (Glaser, 2001; Ouvrard & Price, 2004; Payne, Rowe, Roberts, Charlton, & Docherty, 1999). In addition to single crystal structure determination, Form II is also characterized by melting point, IR and DSC. Crystals of Form II convert to Form I under ambient conditions, however, they are relatively stable at 100 K (Vishweshwar, McMahon, Oliveira, Peterson, & Zaworotko, 2005). DSC thermograms reveal an endothermic peak at 139 °C for Form II in Fig. 5B.

In this study, we have examined the existence forms of PRO and ASA in RPO–ASA combined drugs loaded chitosan nanoparticles by DSC analysis. Fig. 5C shows a melting endothermic peak at 120 °C, which is consist with Fig. 5A. This phenomenon demonstrates that PRO formulated in the ASA–PRO combined drugs loaded chitosan nanoparticles exists in a crystalline phase. Pure ASA shows a melting endothermic peak at 139 °C (Fig. 5B), whereas no peak is detected at the range from 135 to 140 °C for the ASA–RPO combined drugs loaded chitosan nanoparticles (Fig. 5C). ASA is hydrophilic, and the ionic interactions are occurring in the combined drugs loaded chitosan nanoparticles, which include (i) ionic cross-linking between ammonium ion (NH_3^+) of chitosan and carboxylate ion (COO^-) of ASA, (ii) hydrogen bonding between H^+ of carboxylic group of ASA and OH^- of chitosan, and (iii) hydrogen bonding between H^+ of chitosan and OH^- of carboxylic group of ASA. The ionic bond between ammonium ion (NH_3^+) of chitosan and carboxylate ion (COO^-) of ASA is the strongest one formed, which demonstrates that ASA formulated in the combined drugs loaded chitosan nanoparticles exists in an amorphous or disordered crystalline phase or a solid solution state (Smitha, Sridhar, & Khan, 2004; Zhang & Feng, 2006).

3.2. LC and EE of ASA and PRO within chitosan nanoparticles

A comparison of two model drugs encapsulation efficiencies and loading capacities for combined drugs loaded chitosan nanoparticles is shown in Table 1.

Various conditions of effects on encapsulation efficiencies and loading capacities of PRO and ASA have been discussed, including TPP pH value, TPP concentration, ASA initial concentration, PRO initial amount and chitosan MW. (i) When TPP solution is neutral (pH 7) or weak acidic (pH 5), it is disadvantaged for drug encapsulation. Basic (pH 8.6) and strong acidic (pH 3) TPP solutions lead to better encapsulation. Both low and high pH value of TPP contribute to the formation of nanoparticles and the encapsulation of drugs.

Table 1
Encapsulation efficiency and loading capability of chitosan nanoparticles

Variables	EE (wt.%)		LC (wt.%)	
	ASA	PRO	ASA	PRO
TPP pH value				
3	59.1±3.2	43.4±1.7	43.4±2.8	13.8±1.7
5	57.3±4.1	37.0±0.9	38.1±1.6	8.9±1.3
7	52.2±3.3	36.9±2.3	35.0±1.7	7.6±0.9
8.6	68.5±2.1	62.0±1.9	34.3±1.4	12.4±1.1
TPP concentration (mg/ml)				
1	80.1±4.9	37.2±2.2	61.5±2.7	19.1±0.9
1.5	76.2±4.7	46.3±2.4	50.6±2.4	17.5±0.9
2	74.5±4.3	57.2±2.8	42.3±2.1	15.3±0.7
2.5	68.5±3.8	62.0±3.0	34.3±1.6	12.4±1.0
ASA initial concentration (mg/ml)				
0.8	69.6±3.3	62.7±2.5	27.4±1.2	13.1±1.2
1	68.5±3.1	62.0±2.3	34.3±1.5	12.4±1.1
1.2	63.0±2.8	61.5±2.1	37.8±1.7	12.3±1.1
PRO initial amount (mg)				
7.5	71.9±2.6	57.9±2.1	35.9±1.9	8.7±0.8
10	68.5±2.1	62.0±2.7	34.3±2.5	12.4±0.8
12.5	70.0±2.3	37.8±1.8	35.0±2.2	9.4±0.9
Chitosan MW (kDa)				
210	60.1±3.0	69.9±3.4	30.0±0.9	14.0±0.6
400	65.8±4.3	64.5±3.2	32.9±0.8	12.9±0.5
670	68.5±4.4	62.0±0.9	34.3±0.9	12.4±0.6

(ii) With increasing TPP concentration, ASA encapsulating efficiency decreases but encapsulation efficiency of PRO increases, and the loading capacities of the two drugs both decrease. (iii) Encapsulation efficiency and loading capacity of the nanoparticles are affected by the initial ASA concentration and PRO amount in the chitosan solution. The increase of ASA concentration leads to a decrease of ASA encapsulation efficiency and an enhancement of loading capacity; however, it has little effect on PRO. Equally, the increase of PRO concentration also has little effect on encapsulation efficiency and loading capacity of ASA. However, when PRO initial amount is 10 mg, encapsulation efficiency and loading capacity of the PRO reach the optimum value. (iv) The encapsulation efficiency and loading capacity of drugs are not significantly affected by chitosan MW. With increasing chitosan MW, the encapsulation efficiency and loading capacity of ASA increase slightly but the EE and LC of PRO decrease slightly. In all, the EE and LC of ASA and PRO are affected greatly by TPP pH value, TPP concentration and the drugs themselves. These results are probably related to related to the size of combined drug loaded chitosan nanoparticles and interactions between drugs and the combined drugs loaded chitosan nanoparticles. ASA is hydrophilic, and the ionic interactions are occurring in the combined drugs loaded chitosan nanoparticles, instead, PRO is hydrophobic and PRO formulated in the chitosan nanoparticles exist in a crystalline form.

3.3. In vitro release of ASA and PRO from the combined drugs loaded chitosan nanoparticles

Charge density is an important factor in electrostatic interaction and mainly depends on solution pH. The charge of TPP and chitosan are related to solution pH, as well as electrostatic cross-linking of anions to chitosan. Fig. 6A and B shows release behaviors of ASA and PRO from combined drugs loaded chitosan nanoparticles, which are prepared with TPP solutions at various pH levels, respectively.

It is apparent that ASA and PRO release in vitro show very rapid initial bursts. The release profiles of ASA and PRO from combined drug loaded chitosan nanoparticles prepared with TPP solutions of pH 7 and pH 5 show that the release kinetics of two kinds of

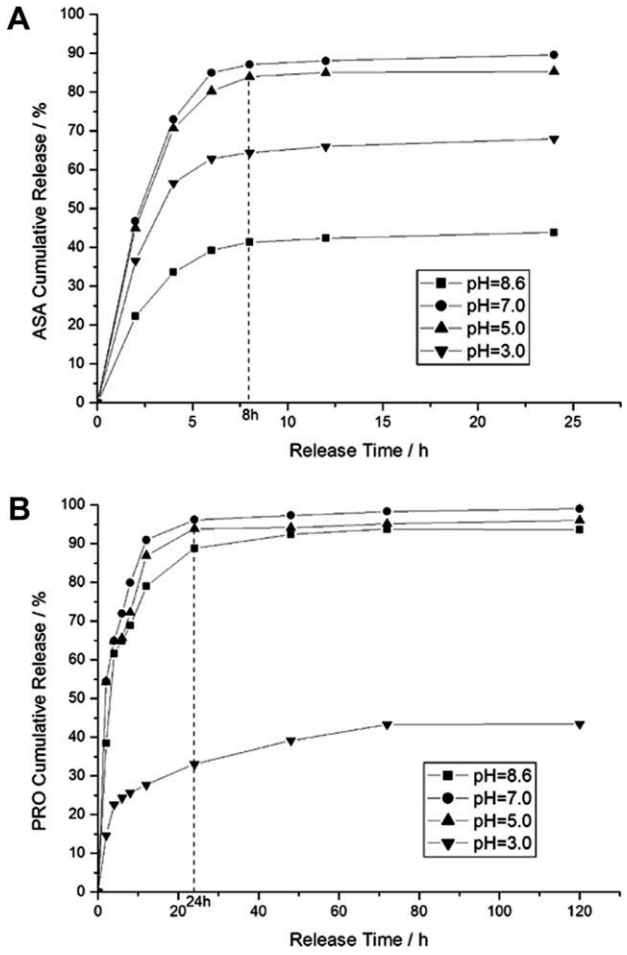

Fig. 6. The influences of TPP pH on ASA (A) and PRO (B) release behaviors.

drug have the same tendency. After 24 h, the percentage release of the two model drugs are about 90%. The difference between two drugs release behaviors lay in that the release rate of PRO (Fig. 6B) is much slower than that of ASA (Fig. 6A) at the beginning, whereas, after 8 h, the release percent of PRO becomes higher than that of ASA. In 8 h, release percents of ASA and PRO reach 83% and 72% (for pH 5), however, release percents of ASA and PRO increase at 85% and 95% in 24 h, respectively. Compared with ASA release behavior, the change of release percent of PRO becomes more noticeable from 8 to 24 h, which is due to the difference of the release mechanisms of ASA and PRO. ASA is hydrophilic and easily diffuses from nanoparticles, instead PRO is only released from nanoparticles collapsing, so in the initial 8 h, the release percent of PRO is lower than that of ASA, on the contrary, the release percent of PRO is higher than that of ASA from 8 to 24 h. Much difference is also found in release percent of the two drugs from nanoparticles prepared with different TPP solutions. As shown in Fig. 6A, strong acidic (pH 3) and basic TPP solution (pH 8.6) lead to a decrease of ASA release rate. About 64% and 40% of ASA are released from nanoparticles within 8 h, respectively. By contrast, when the TPP is neutral or near neutral (pH 7 or 5), the significantly faster releases of ASA are achieved, with releases of 87% and 83% after 8 h, respectively. However, unlike ASA, strong basic TPP does not decrease PRO release rate a lot, but only strong acidic (pH 3) TPP solutions makes for a big decrease in PRO release rate. The release rates of ASA and PRO are adjusted by changing the TPP pH values. ASA and PRO release fast when TPP solution is neutral, and with the TPP pH deviating from neutral, ASA and PRO release become slow. It is believed that basic and acidic TPP solution is more convenient for the nanoparticles formed as high ionization degree. The sufficient cross-linking between TPP polyanion and amino groups of chitosan makes the nanoparticles in high density structure, consequently, the drugs release slowly. This is consistent with the result for encapsulation efficiency and loading capacity of ASA and PRO at the same pH.

Fig. 7A and B shows the effects of the cross-linking agent (TPP) concentration on ASA and PRO release. In general, the release rates of the two model drugs from the drug loaded chitosan nanoparticles increase with increasing cross-linking agent concentration. With the change of TPP solution concentration as 1.0, 1.5, 2.0 and 2.5 mg/mL, the release percent of ASA after 8 h is 22%, 43%, 59%, 87% and the release percent of PRO is 28%, 41%, 54% and 69%, respectively. With increasing TPP concentration, the size of the chitosan nanoparticles apparently increase. The nanoparticles are eroded more quickly in PBS buffer with increasing size. This makes the particles rapidly lose their integrity and results in rapid drug release.

The effect of the loading of one drug on the release from the two drug system was studied. Fig. 8 shows the release profiles of ASA and PRO with different initial concentration, respectively. In brief, the effect of different initial ASA concentration on its release is less. For an initial ASA concentration of 0.8, 1.0 and 1.2 mg/mL, the release percent of ASA is 56%, 61% and 68%, respectively, within 4 h (Fig. 8A). When the initial ASA concentration is 1.0 and 1.2 mg/mL, the difference between two release profiles of PRO can be ig-

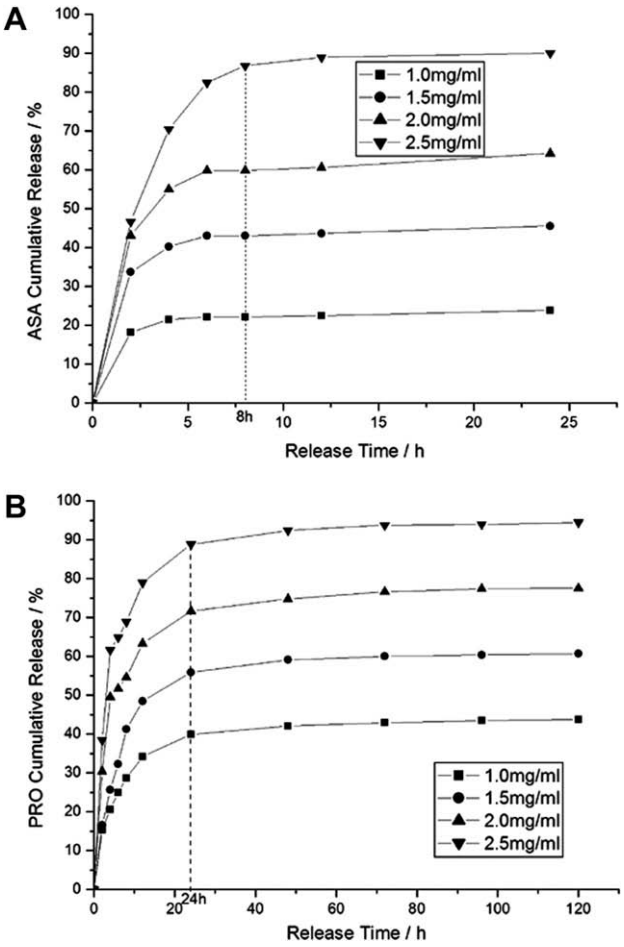

Fig. 7. The influences of the TPP concentration on ASA (A) and PRO (B) release behaviors.

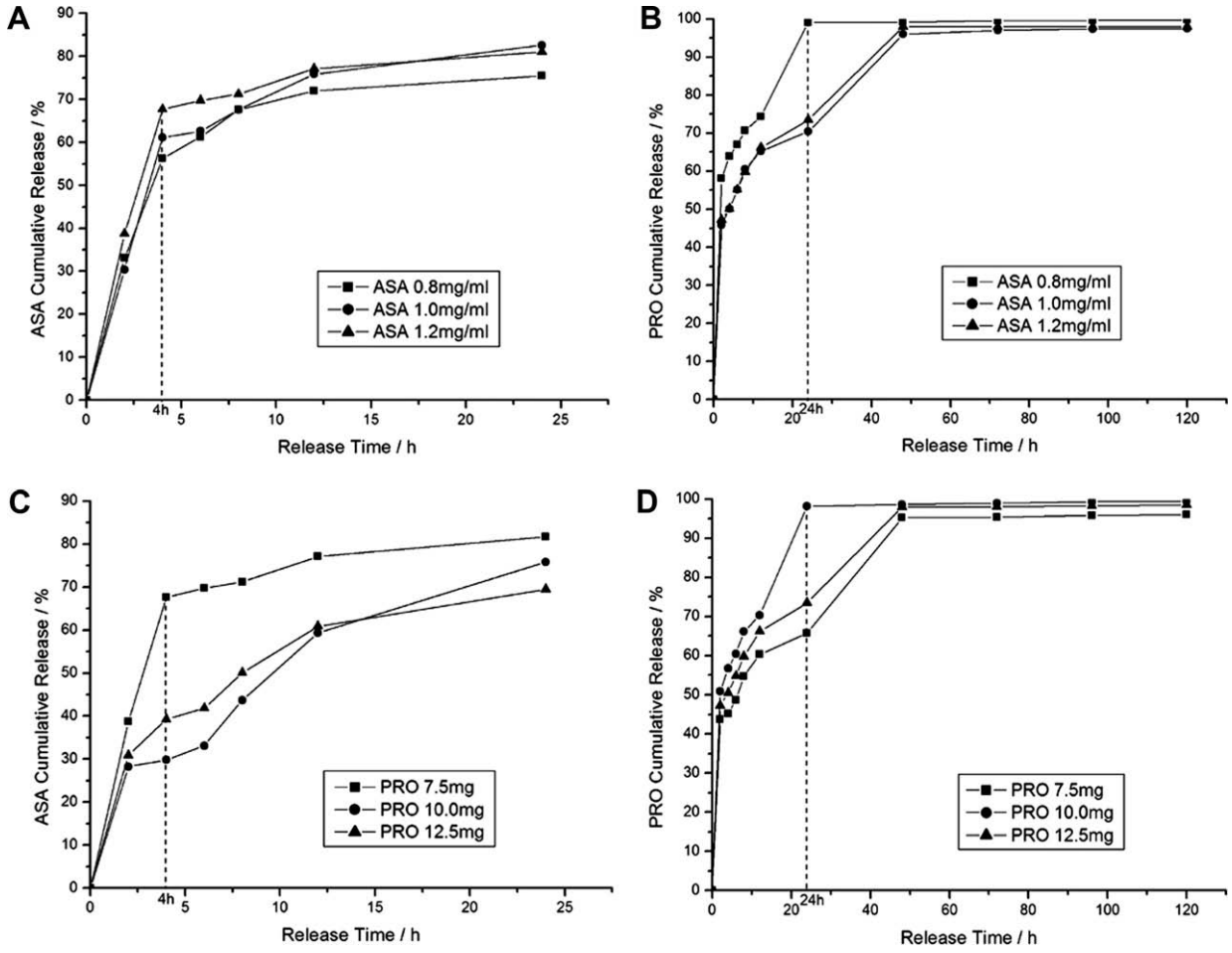

Fig. 8. The influences of ASA and PRO initial concentrations on two drugs release behaviors: ASA on ASA (A), ASA on PRO (B), PRO on ASA (C) and PRO on PRO (D).

nored. But as the initial ASA concentration is 0.8 mg/mL, the release profile of PRO shows a very rapid initial burst (Fig. 8B).

The influences of initial PRO amount on ASA and PRO release profiles are showed in Fig. 8C and D. After 4 h, the effect on ASA release percent is clear when the initial PRO amount is 7.5, 10.0 and 12.5 mg, the release percent of ASA is 67%, 30% and 39%, respectively. The PRO release speed changes little, except that the release percent is 98% after 24 h when the initial PRO amount is 10.0 mg.

Based on the data discussed above, two drugs release profiles are not significantly affected by their own initial loading amount, which might be attributed to the different loading modes. As mentioned, ASA is loaded on the chitosan nanoparticles because of blending and electrostatic interaction between its carboxyl and amino groups of chitosan. However, PRO is physically entrapped in the nanoparticles.

Fig. 9 shows the influences of chitosan MW on the ASA and PRO releases. The viscosity of chitosan solution is important for the formation of nanoparticles. As the MW of the chitosan increases, the release behavior of ASA decreases significantly (Fig. 9A). The release of ASA is faster from the nanoparticles that prepared with 210 kDa chitosan than those made from 400 kDa chitosan. These results indicate that the release behaviors of ASA depend on the viscosity of the chitosan solution. The increased viscosity of chitosan solution forms relatively strong walls of nanoparticles upon interaction with TPP. High cross-linking density of TPP–chitosan matrix results in less swelling ability, therefore the release of ASA decreases. By contrast, the influence of chitosan MW on PRO release is almost negligible (Fig. 9B). These clear differences could be attributed to different loading mechanisms and release mechanisms of the two drugs. ASA is hydrophilic, and interacts ionically with the chitosan nanoparticles, and is physically entrapped in the chitosan nanoparticles. ASA diffuses easily from the nanoparticles while PRO diffuses only with difficulty. Nanoparticles disruption being required to accelerate release.

4. Conclusions

We report the successful preparation of combined drugs loaded chitosan nanoparticles achieved by combining ASA and PRO. The physical forms of two drugs in the polymer are characterized. PRO formulated in nanoparticles exists in a crystalline phase and ASA exists in an amorphous or disordered crystalline phase or a solid solution state because of blending and electrostatic interaction between its carboxyl and amino groups of chitosan. It is found that the encapsulation efficiency and loading capacity of ASA and PRO are affected greatly by TPP pH value, TPP concentration and drugs themselves. In addition, the release rates of ASA and PRO are dependent on the pH and concentration of TPP. In addition, the release rate of ASA depends on chitosan molecular weight, by contrast, the release rate of PRO is independent of chitosan molecular weight. As different loaded mode, the influences of the initial drugs amount on their release are apparent. In the future, this work will have implications in the design of vehicles for loading several drugs at the same time and therapy to solve the prob-

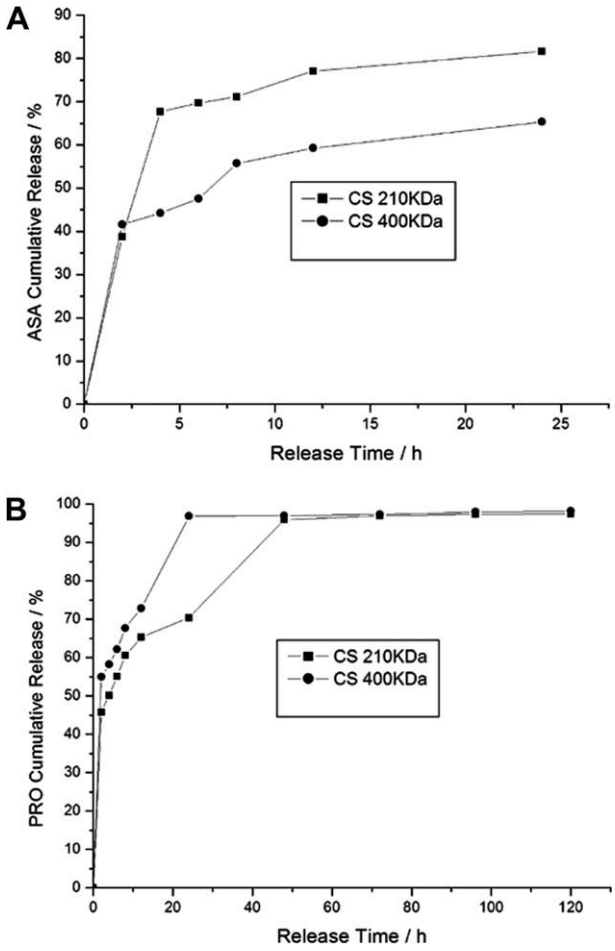

Fig. 9. The influences of chitosan MW on ASA (A) and PRO (B) release behaviors.

lem of complexity of restenosis pathogenesis effectively. Last, this study may be helpful for nanoparticles loaded ASA/PRO clinic application and offer the instructive reference to ASA/PRO clinic combination dosing.

Acknowledgements

This work is supported by the National Natural Science Foundation of China (Grant Nos. 20376045, 20676079), and partly supported by the Nanometer Technology Program of Science and Technology Committee of Shanghai (0452nm037).

References

Baim, D. S. (1992). Interventional catheterization techniques: Percutaneous transluminal balloon angioplasty, valvuloplasty and related procedures. In E. Braunwald (Ed.), *Heart disease: A textbook of cardiovascular medicine* (pp. 1365–1381). Philadelphia: Saunders.

Banai, S., Chorny, M., Gertz, S. D., Fishbein, I., Gao, J., Perez, L., et al. (2005). Locally delivered nanoencapsulated tyrphostin (AGL-2043) reduces neointima formation in balloon-injured rat carotid and stented porcine coronary arteries. *Biomaterials, 26*, 451–461.

Banai, S., Wolf, Y., Golomb, G., Pearle, A., Waltenberger, J., & Fishbein, I. (1998). PDGF-receptor tyrosine kinase blocker AG1295 selectively attenuates smooth muscle cell growth in vitro and reduces neointimal formation after balloon angioplasty in swine. *Circulation, 97*, 1960–1969.

Broman, E., Khoo, C., & Taylor, L. S. (2001). A comparison of alternative polymer excipients and processing methods for making solid dispersions of a poorly water soluble drug. *International Journal of Pharmaceutics, 222*, 139–151.

Calvo, P., Remuñán-López, C., Vila-Jato, J. L., & Alonso, M. J. (1997). Novel hydrophilic chitosan-polyethylene oxide nanoparticles as protein carriers. *Journal Applied Polymer Science, 63*, 125–132.

Currier, J. W., & Faxon, D. P. (1995). Restenosis after percutaneous transluminal coronary angioplasty: Have we been aiming at the wrong target? *Journal of the American College of Cardiology, 25*, 516–520.

Fang, S. Q., Wang, W. X., Lu, H. M., Huang, F. L., Guo, L. M., Hong, X., et al. (1999). The chemical structure and test on relative substances of probucol. *Chinese New Drugs Journal, 8*, 1999–2002.

Fishbein, I., Chorny, M., Banai, S., Levitzki, A., Danenberg, H. D., & Gao, J. (2001). Formulation and delivery mode affect disposition and activity of tyrphostin-loaded nanoparticles in the rat carotid model. *Arteriosclerosis, Thrombosis, and Vascular Biology, 21*, 1434–1439.

Fishbein, I., Chorny, M., Rabinovich, L., Banai, S., Gati, I., & Golomb, G. (2000). Nanoparticulate delivery system of a tyrphostin for the treatment of restenosis. *Journal of Controlled Release, 65*, 221–229.

Gerber, J. J., Caira, M. R., & Lotter, A. P. (1993). Structures of two conformational polymorphs of the cholesterol-lowering drug probucol. *Journal of Crystallographic and Spectroscopic Research, 23*, 863–869.

Glaser, R. (2001). Aspirin. An ab initio quantum-mechanical study of conformational preferences and of neighboring group interactions. *Journal of Organic Chemistry, 66*, 771–779.

Guzman, L. A., Labhasetwar, V., Song, C., Jang, Y., Lincoff, A. M., & Levy, R. (1996). Local intraluminal infusion of biodegradable polymeric nanoparticles. A novel approach for prolonged drug delivery after balloon angioplasty. *Circulation, 94*, 1441–1448.

Janes, K. A., Calvo, P., & Alonso, M. J. (2001). Polysaccharide colloidal particles as delivery systems for macromolecules. *Advanced Drug Delivery Reviews, 47*, 83–97.

Joseph, J. G. (2006). Polymers for tissue engineering, medical devices, and regenerative medicine. Concise general review of recent studies. *Polymers for Advanced Technologies, 17*, 395–418.

Kato, M., Azuma, H., Akaike, M., Iuchi, T., Aihara, K., Ikeda, Y., et al. (2005). Aspirin inhibits thrombin action on endothelial cells via up-regulation of aminopeptidase N/CD13 expression. *Atherosclerosis, 183*, 49–55.

Knaul, J. Z., Hudson, S. M., & Creber, K. A. M. (1999). Improved mechanical properties of chitosan fibers. *Journal of Applied Polymer Science, 72*, 1721–1731.

Ko, J. A., Park, H. J., Hwang, S. J., Park, J. B., & Lee, J. S. (2002). Preparation and characterization of chitosan microparticles intended for controlled drug delivery. *International Journal of Pharmaceutics, 249*, 165–174.

Koleva, B. B. (2006). Polymorphs of aspirin – Solid-state IR-LD spectroscopic and quantitative determination in solid mixtures. *Journal of Molecular Structure, 800*, 23–27.

Kolhe, P., & Kannan, R. M. (2003). Improvement in ductility of chitosan through blending and copolymerization with PEG: FTIR investigation of molecular interactions. *Biomacromolecules, 4*, 173–180.

Lee, S. T., Mi, F. L., Shen, Y. J., & Shyu, S. S. (2001). Equilibrium and kinetic studies of copper(II) ion uptake by chitosantripolyphosphate chelating resin. *Polymer, 42*, 1879–1892.

Li, J., Yun, H., Gong, Y., Zhao, N., & Zhang, X. (2006). Investigation of MC3T3–E1 cell behavior on the surface of GRGDS-coupled chitosan. *Biomacromolecules, 7*, 1112–1123.

Lim, S. H., Park, K. S., Park, H. S., Gin, Y. J., Noh, I. S., Park, C. W., et al. (2005). Influence of heat treatment on biological properties of chitosan toward vascular cells in vitro. *Macromolecular Symposia, 224*, 263–273.

Madihally, S. V., & Matthew, H. W. T. (1999). Porous chitosan scaffolds for tissue engineering. *Biomaterials, 20*, 1133–1142.

Mi, F. L., Shyu, S. S., Kuan, C. Y., Lee, S. T., Lu, K. T., & Jang, S. F. (1999a). Chitosan-polyelectrolyte complexation for the preparation of gel beads and controlled release of anticancer drug. I. Enzymatic hydrolysis of polymer. *Journal of Applied Polymer Science, 74*, 1868–1879.

Mi, F. L., Shyu, S. S., Lee, S. T., & Wong, T. B. (1999b). Kinetic study of chitosan–tripolyphosphate complex reaction and acid-resistive properties of the chitosan-tripolyphosphate gel beads prepared by in-liquid curing method. *Journal of Polymer Science Part B: Polymer Physics, 37*, 1551–1564.

Nobuyoshi, M., Kimura, T., & Ohishi, H. (1991). Restenosis after percutaneous transluminal coronary angioplasty: Pathologic observation in 20 patients. *Journal of the American College of Cardiology, 17*, 433–439.

Ouvrard, C., & Price, S. L. (2004). Toward crystal structure prediction for conformationally flexible molecules: The headaches illustrated by aspirin. *Crystal Growth and Design, 4*, 1119–1127.

Payne, R. S., Rowe, R. C., Roberts, R. J., Charlton, M. H., & Docherty, R. J. (1999). Potential polymorphs of aspirin. *Journal of Computational Chemistry, 20*, 262–273.

Qi, L. F., & Xu, Z. R. (2004). Lead sorption from aqueous solutions on chitosan nanoparticles. *Colloids Surfaces A: Physicochemical Engineering Aspects, 251*, 183–190.

Qi, L. F., & Xu, Z. R. (2006). In vivo antitumor activity of chitosan nanoparticles. *Bioorganic and Medicinal Chemistry Letters, 16*, 4243–4245.

Qi, L. F., Xu, Z. R., Jiang, X., Hu, C. H., & Zou, X. F. (2004). Preparation and antibacterial activity of chitosan nanoparticles. *Carbohydrate Research, 339*, 2693–2700.

Qi, L. F., Xu, Z. R., Jiang, X., Li, Y., & Wang, M. Q. (2005). Cytotoxic activities of chitosan nanoparticles and copper-loaded nanoparticles. *Bioorganic and Medicinal Chemistry Letters, 15*, 1397–1399.

Smitha, B., Sridhar, S., & Khan, A. A. (2004). Polyelectrolyte complexes of chitosan and poly(acrylic acid) as proton exchange membranes for fuel cells. *Macromolecules, 37*, 2233–2239.

Thierry, B., Winnik, F. M., Merhi, Y., Silver, J., & Tabrizian, M. (2003). Bioactive coatings of endovascular stents based on polyelectrolyte multilayers. *Biomacromolecules, 4*, 1564–1571.

Vishweshwar, P., McMahon, J. A., Oliveira, M., Peterson, M. L., & Zaworotko, M. J. (2005). The predictably elusive form II of aspirin. *Journal of the American Chemical Society, 127*, 16802–16803.

Watanabe, K., Sekiya, M., Ikeda, S., Miyagawa, M., & Hashida, K. (1996). Preventive effects of probucol on restenosis after percutaneous transluminal coronary angioplasty. *American Heart Journal, 132*, 23–29.

Zhang, Z. P., & Feng, S. S. (2006). In vitro investigation on poly(lactide)-Tween 80 copolymer nanoparticles fabricated by dialysis method for chemotherapy. *Biomacromolecules, 7*, 1139–1146.